13

Factors determining parasitic thermionic current in cathode-grid units with pyrographite grids

© R.Yu. Bogachev,[1,2] T.M. Krachkovskaya,[1] V.I. Shesterkin,[1] S.D. Zhuravlev,[1] O.E. Glukhova,[1,3,4] D.A. Kolosov[1,3]

[1]Joint Stock Company Research and Production Enterprise Almaz, Saratov, Russia
[2]Yuri Gagarin State Technical University of Saratov, Saratov, Russia
[3]Saratov National Research State University, Saratov, Russia
[4]I.M. Sechenov First Moscow State Medical University, Moscow, Russia
e-mail: bogachevru@almaz-rpe.ru

Received October 4, 2024
Revised January 18, 2025
Accepted January 30, 2025

The article presents the results of studying the grid electrodes made of anisotropic pyrolytic graphite (APG) as part of the cathode-grid unit (CGU) of a powerful pulsed traveling-wave tube (TWT). It was found that the grid electrodes made of APG demonstrated high anti-emission properties in the temperature range of 800 °C–900 °C at cathode temperatures of 1080 °C–1150 °C. It was found that during testing the CGU as part of a TWT device for 900 hours in the forced mode (the cathode temperature exceeded the operating temperature by 70 °C), there was no parasitic thermionic current in the cathode-control grid circuit. This result can be explained by an increase in the electron work function of the APG with a barium oxide film adsorbed on its surface. The results of calculations using the density functional method and quantum molecular dynamics modeling for the structure of APG with a BaO film having a hexagonal lattice showed that the value of its electron work function was ~ 5.14 eV, which is significantly higher than the work function of APG (~ 4.7 eV) and barium oxide ($\sim 1-1.6$ eV).

Keywords: parasitic thermal emission, cathode-grid unit, anisotropic pyrolytic graphite, density functional theory, adsorption, molecular dynamics modeling.

DOI: 10.61011/TP.2025.06.61385.312-24

Introduction

Low-voltage control of the electron beam current in pulsed TWT is carried out by the potential of a grid located at a distance of $100-300\,\mu$m from the emitting surface of the cathode. Current-tapping grids are used in TWT of X-range with an average output power level of no more than 50–60 W. In more powerful TWT, under the influence of the power of the electron beam tapped by the grid, the „parasite“ current of thermionic emission from the grid exceeds the permissible values, and its junctions deform or collapse. The tapping of current by the control grid jumpers is eliminated by placing a shadow grid between the control grid and the cathode, located near the surface and having a cathode potential, directly on the surface of the cathode (connected grid) or in the body of the cathode tablet (built-in grid) [1].

Grid structures operate in vapors of the products evaporated from the surface of a metal-porous cathode (MPC), which are adsorbed on the surface of the grid and change the electron's work function [2,3]. At a temperature of 1100 °C–1200 °C in the first 100–200 h BaO makes the 95 % of the evaporated active substance. Further, during the operation of the cathode, the ratio of Ba and BaO in the active substance evaporated from the cathode surface is 90 %/1 % [4,5]. When a film of a certain thickness is formed, the electron work function when leaving the grid surface is determined by the composition of the adsorbed substance and may be significantly less than the electrons work function of the pure grid material, which increases the current density of parasitic thermoelectric emission from its surface [3].

Hafnium sheet is used as the material of the grid electrodes in the cathode-grid knots of klystrons and high-power pulsed TWT, which does not adversely affect the emission of MPC and is featuring satisfactory mechanical and anti-emission properties. The disadvantages of hafnium include a decrease in shape stability and its recrystallization at 950 °C–1100 °C, which is close to the operating temperature of the grids in the composition of vacuum electronic devices (VED). A decrease in the shape stability of hafnium grids leads to a violation of the shielding of the control grid jumpers, an increase in its temperature due to the power of the tapped electron flux and, as a result, to an increase in the current of parasitic thermionic emission from the control grid in the pause between pulses, which reduces the durability and reliability of TWT [2,6].

Therefore, the use of grid electrodes made of materials with higher dimensional stability and anti-emission properties in CGK is an urgent task [6].

Alternative materials of the grid structures with high anti-emission properties include various carbon modifications or traditionally used metals (Hf, Mo and etc.) with carbon coatings [1,7–12].

Among the materials with a high work function, chemical inertia, stable mechanical properties at temperatures

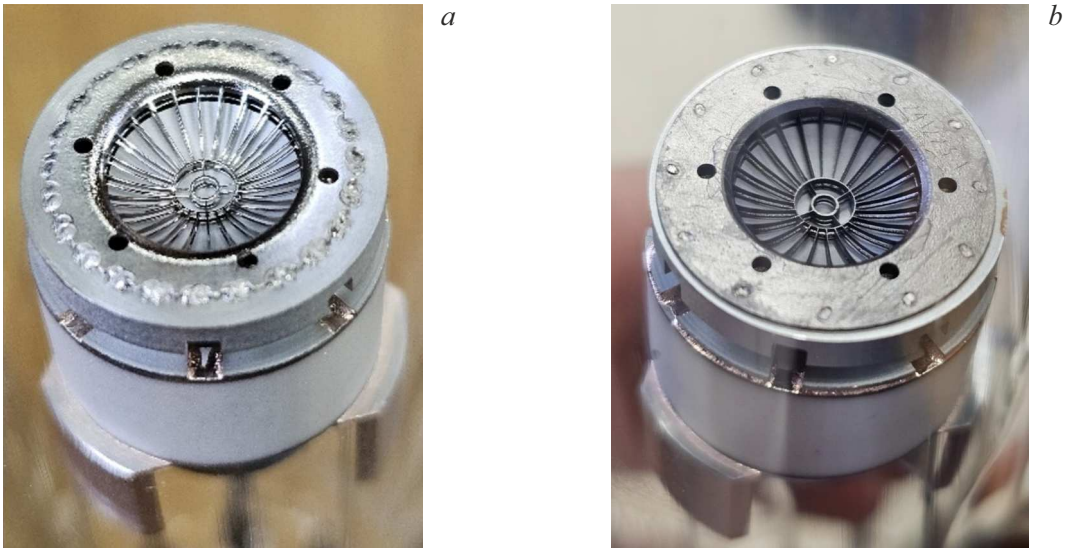

Figure 1. General view of CGK complete with open-work grids made of hafnium (*a*) and of APG (*b*).

900 °C–1000 °C during the required service life and without adversely affecting the emission characteristics of MPC is anisotropic pyrolytic graphite (APG) [10–12].

The purpose of this paper is an experimental study of the dynamics of time variation of a parasitic thermionic current in a CGK with dual (control and shadow) grid structures made of APG as part of a powerful pulsed TWT and a theoretical study of the work function and energy of Ba and BaO binding to APG surface.

1. Grid structures made of APG

For the manufacture of grid structures (shadow and control), APG blanks were used synthesized by pyrolytic deposition of carbon atoms onto graphite substrates heated to a temperature of 1800 °C of MPG6 grade by dissociation of carbon-containing gases (methane, heptane) at a temperature of 2000 °C–2500 °C. Thickness of the shadow grid blanks makes 100 μm, thickness of control grid — 300 μm. The parts obtained in this way have anisotropy of the basic thermal and electrical properties in the direction of layers deposition and perpendicular to them, as well as in terms of thermal linear expansion (TLE) coefficient and strength. The content of impurities in the material, determined by X-ray diffraction and X-ray fluorescence analysis, is less than 0.01%, and the shape and dimensions of the deposition substrate determine the shape and dimensions of the parts obtained and do not require additional mechanical treatment.

X-ray diffraction analysis of the crystal structure of APG plate, performed using a multifunctional X-ray diffractometer DRON-8T, showed that the sample itself is a highly textured graphite with a unit cell parameter $c = (6.82228 \pm 0.00017)$ Å.

Moreover, the TLE coefficient of APG in the direction of deposition plane was found with its value equal $18.5 \cdot 10^{-7}\,\mathrm{K}^{-1}$, which is 3.3 times less than that of Hafnium.

The work [13] presents the results of changes in the interelectrode distances in CGK by the high-power pulsed TWT with hafnium grids caused by thermal displacement of the cathode and grid structures relative to its cold state. With the cathode working temperature of 1080 °C the cathode shifted towards the control grid at 61 μm, and the control grid shifted towards the cathode at — 12 μm. Since CGKs with grids made of Hafnium and APG are identical, the shift of APG grid towards cathode doesn't exceed 3.6 μm which leads to higher current of the cathode with a diameter of 10 mm that according to „three-halves-power law" will increase by no more than 3.4 %.

Thus, the use of APG grids instead of hafnium as a material will reduce the value of the parasitic thermoemission current from the control grid, leakage current through ceramics, and direct tapping current.

2. Testing of electron guns with APG grids

CGK with APG grids for high-power pulsed TWT were fabricated using laser ablation technologies for fastening and stitching double grid structures [14,15].

The CGK with APG grids as a part of a powerful TWT were studied. These CGKs had a structure shown in Fig. 1. Parameters of CGK in TWT are listed in Table 1.

CGK devices with APG grids were dynamically tested at depths from 40 to 4 in accordance with the technical specifications for this device, during which there were no any ohmic leaks in the cathode-control grid circuit and parasitic thermoelectronic emission current. At the next stage, the devices successfully passed a test cycle for vibration and impact resistance according to the method

Table 1. Parameters of CGK in TWT

Diameter of cylindrical part of cathode, mm	10
Cathode current in pulsed mode, A	4
Operating temperature of cathode, °C	1055–1080
Grid locking voltage, V	no less than −320
Grid overvoltage, V	no more +750
Anode voltage, V	21000–22000
Minimal off-duty ratio	4

established for commercial devices with a one-and-a-half-fold acceleration margin to provide additional technological reserve to withstand mechanical impact [1]. The change in parameters of the amplitude of modulation of the output signal and the output pulse power after completion of vibration resistance tests does not exceed the permissible values of 8% and 3%, respectively, which meets the requirements of the technical specifications for this device.

At the final stage of testing the CGK devices with APG grids passed the test in „continuous ignition" mode (with continuously supplied incandescence voltage without drawn current) at high cathode temperature of 1150 °C (acceleration coefficient 7 relative to the working temperature): the first devices during 900 h and the second one during 400 h with control of underheating at the off-duty ratios of 10 and 4 every 100 h. During the testing time in extreme grid conditions — under temperature exposure and a minimum off-duty ratio of 4 — the current values in the cathode-control grid circuit remained unchanged relative to the start of the tests and amounted to −0.01 mA for the first and −0.05 mA for the second device. Permissible current in the grid circuit was no more than −0.75 mA.

3. Study of chemical composition of a substance adsorbed on grid electrodes

After the end of the tests on a scanning electron microscope, the surfaces of shadow and control APG grids were examined. Surface analysis confirmed the presence of sputtering from the cathode onto the jumpers surfaces facing it.

Figures 2, 3 show photos of the surfaces of the shadow and control grids facing the cathode, with a significant amount of adsorbed evaporation products from the surface of the MPC. The evaporation products are unevenly distributed over the grids surface. Along with relatively clean areas in the area of the central ring, the film thickness of the adsorbed substance on the radial jumpers increased from the center to the periphery of the grids.

X-ray diffraction analysis revealed a significant amount of evaporation products from the cathode's tungsten sponge (Ba, O, Ca, Al) on the surfaces of both grids facing the cathode. Chemical elements of the coating of the cathode emitting surface of (Os, Ir) film were found, especially in the central part of the grids, which are usually not detected during the study after testing of hafnium grid CGKs with an operating time of less than 100 h, solder elements of the cathode knot (Co, W) and electrode block solder (Cu) (Table 2).

Despite the significant amount of adsorbed evaporation products from the cathode, during the long-term operation of the devices in TWT with APG grids at elevated cathode temperature and off-duty ratio from 100 to 4, no parasitic current of thermionic emission was recorded.

The results obtained confirm the prospects of using APG as a grid structure for high-power microwave electrovacuum devices.

4. Theoretical study of the interaction of barium and barium oxide with the surface of APG grids

The theoretical study of the effect of barium and barium oxide adsorbed on APG surface on the magnitude of the electron work function and the bond energy was carried out using the density functional theory (DFT) method in Siesta software [16]. The pseudopotentials for carbon, barium, and oxygen atoms were taken from Simune database [17]. The exchange-correlation interaction was delineated by method of the generalized gradient approximation (GGA) in Perdew–Burke–Ernzerhof (PBE) formualtion [18]. Van der Waals interaction of graphene layers as part of APG was simulated using DFT-D2 correction of Grimme dispersion. Electronic wave functions were constructed as linear combinations of atomically centered basis functions in the full form of DZP (Double Zeta + Polarization) atomic orbitals, including polarization orbitals with a cutoff of 600 Ry. The Monkhorst-Pack approach with a grid $4 \times 4 \times 1$ was used to partition the first Brillouin zone of the inverse space. To study the behavior of „APG + Ba/BaO" system at different temperatures the method of quantum molecular dynamics „Anneal" was used. The variable parameters included all the coordinates of all the cells atoms and the lengths of the translation vectors. The bond energy of barium/barium oxide with APG was calculated as a difference of full energy E_{total} of „APG + Ba/BaO" system and pyrographite energy, and Ba/BaO. The work function W_F of electrons emitted by „APG + Ba/BaO" surface into vacuum was determined as the difference between the energy of the electron E_{vac} (near the surface) and the Fermi energy E_F, and the energy E_{vac} — from electrostatic Poisson equation for a self-consistent field, which took into account the contribution of all ionic cores of the atomic grating.

APG supercell included several graphene layers. The number of layers was determined by a preliminary study of the pattern of the electrons work function variation with an increase in the number of graphene layers in the cell. When five layers or more were reached in the cell, the work function was ~ 4.5 eV, which corresponds to the work

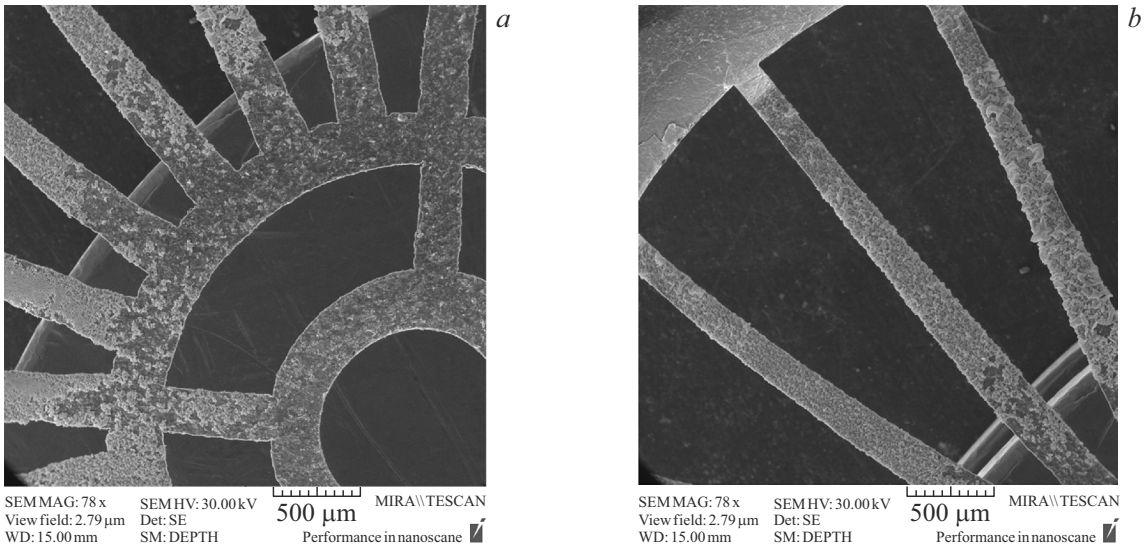

Figure 2. Shadow grid. View from the cathode side: *a* — central part with circular jumpers, *b* — periphery part with radial jumpers.

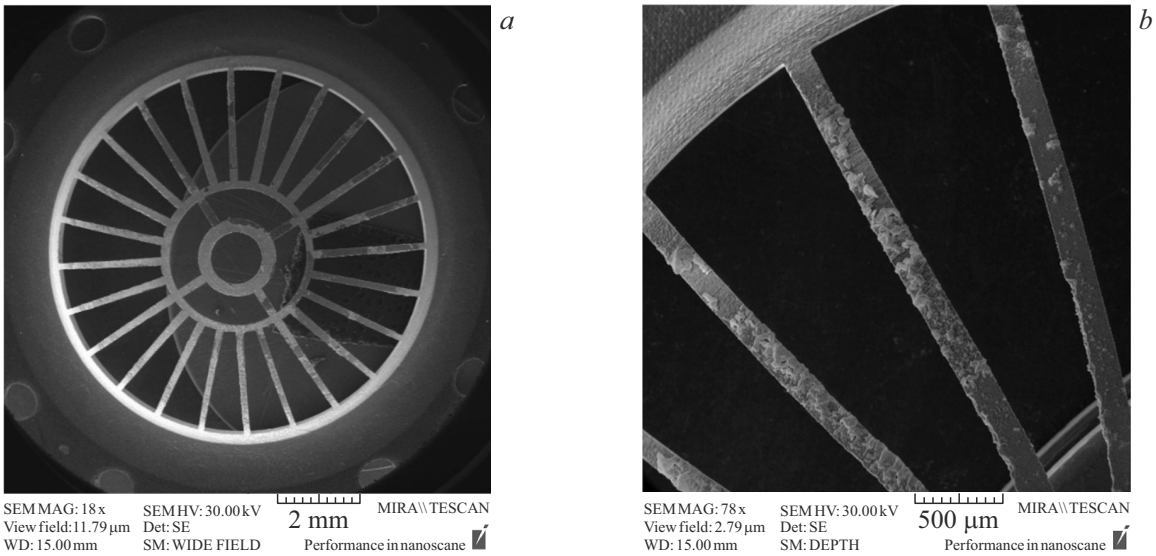

Figure 3. Control grid. View from the cathode side: *a* — general view, *b* — periphery.

Table 2. Chemical composition of the substance adsorbed on the grid electrodes

Chemical element	Sputtering quality on the shadow grid, mass %	Sputtering quantity on the control grid, mass %
Ba	7–71	10.7–61.3
O	7–39	13.59–39.4
Ca	0.81–8	0.6–5.29
Al	0.12–7.24	0.07–11.02
Os	0.39–2.16	0.41–5.5
Ir	0.33–0.85	0.47–1.82
Co	0.31–70	0.89–44.51
W	0–2.44	0–12.33
Cu	0.12–0.4	0.11–0.58

function of graphite. The number of atoms in each layer was chosen in such a way that its dimensions corresponded to the lattice of barium and barium oxide.

Studies have been conducted on the work function variation with an increase in the number of layers of Ba/BaO lattice films on the surface of a five-layer APG. Monolayer crystalline films of Ba and BaO formed a hexagonal structure, repeating the pattern of the surface on which they were adsorbed (Fig. 4, *a, c*, respectively). Their elementary cells with five carbon layers are shown in Fig. 5, *a, b*, layer-by-layer film buildup was carried out up to six atomic layers. The pattern of the work function W_F variation (at 300 K) is illustrated in Fig. 5, *c*. For the adsorbed barium, the trend of W_F variation is expected, since after barium appearance it decreased from 4.49 eV, specific for

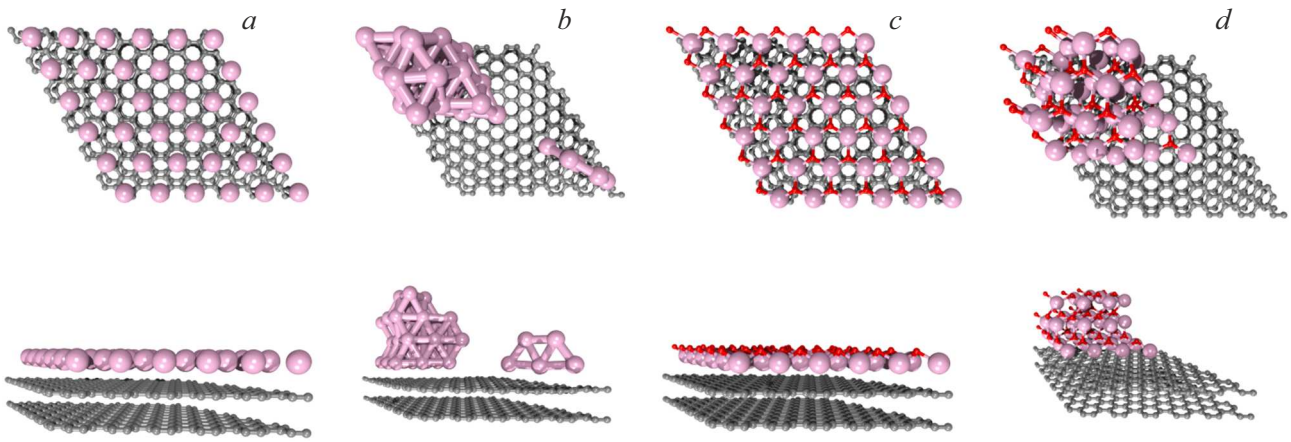

Figure 4. Supercells of atomic film models „APG + Ba/BaO“: *a* — uniform distribution of barium; *b* — non-uniform distribution of barium; *c* — uniform distribution of BaO; *d* — non-uniform BaO distribution (carbon atoms are marked in gray, barium atoms in pink, oxygen atoms are denoted in red). Here, APG has two carbon layers.

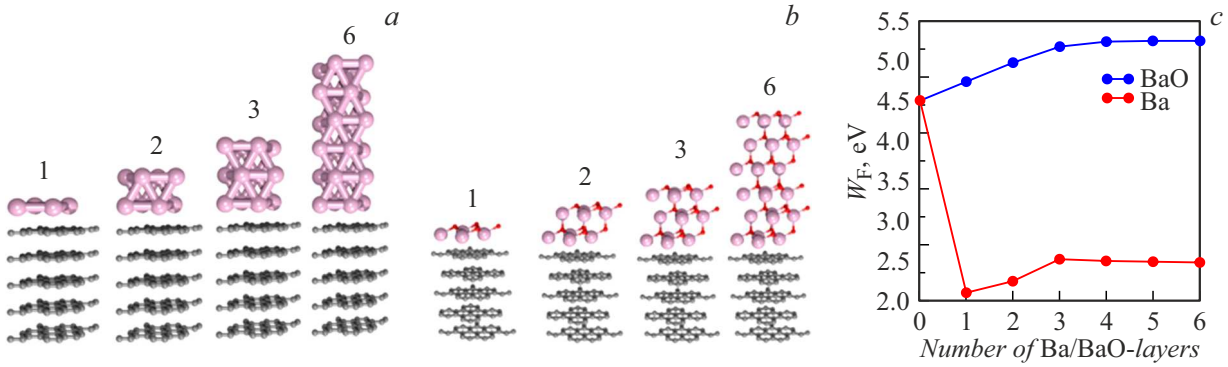

Figure 5. „APG + Ba/BaO“ films: *a* — atomistic cells of the film models „APG + Ba“; *b* — atomistic cells of the film models „APG + BaO“; *c* — graph of the work function variation with increasing number of Ba/BaO layers.

the pyrographite, to 2.16 eV, and then, starting from the third layer to the sixth, it stabilized in consistency with the work function of crystalline barium — 2.5 eV. That it the work function of „APG + Ba“ film is defined by the value W_F of barium. A completely different pattern of W_F variation was discovered for „APG + BaO“ film: as the number of BaO layers increases, the work function increases, reaching 5.14 eV with six layers of barium oxide. To explain this effect, additional studies were carried out, namely, the work function of hexagonal six-layer BaO lattice structure formed on the surface of APG was calculated. Its work function $W_F = 5.41$ eV, which is significantly higher than the work function for the cubic crystal of BaO — 1.61 eV. This explains why the work function of „APG + BaO“ film is much higher than that of pure APG.

First of all, the effect of the heterogeneity of the adsorbed Ba/BaO cluster formations distribution on the work function was investigated. For this purpose, atomic models were constructed containing the same number of carbon and Ba/BaO atoms, uniformly and non-uniformly distributed over the surface. In this case, the supercells of the models included only two graphene layers to reduce the computational resources and calculation time required for DFT-calculations. Fig. 4 illustrates the supercells of the models. In case of a uniform distribution of Ba/BaO, the monoatomic films located at distances of 3.44 and 3.45 Å respectively, are considered (Fig. 4, *a, c*). With a non-uniform distribution of Ba/BaO, fragmentary coatings were formed as separate clusters of various sizes, similar to the data shown in Fig. 2 and 3. The corresponding supercells of the atomistic models are shown in Fig. 4, *b, d*, at that the height of Ba-clusters above the surface of the carbon layer made $\sim 10.1-17.8$ Å, the height of BaO clusters — ~ 14.3Å. Distances of Ba–graphene and BaO–graphene remain practically the same — 3.47 and 3.42 Å. Ba supercells contain 468 atoms (among them 36 Ba-atoms), in case of BaO — 504 atoms (36 Ba-atoms and 36 O-atoms). The bond energy of Ba is 1.57 eV (per barium atom), which is slightly less than the bond energy of barium oxide, which is 2.55 eV (per BaO complex). Calculations of the work function showed that nonuniform Ba distribution leads to an increase of the work function by only 3.7,% from 2.16 to 2.24 eV. The nonuniformity of BaO location also results in higher work function by 2.3 % from 3.87

to 3.96 eV. The experiments were carried out at temperature of 300 K. Thus, the nonuniformity does not significantly affect the work function, therefore, a uniform coating of the carbon structure with adsorbents was further investigated.

The next important step was to study the effect of high temperatures on the behavior of „APG + Ba/BaO“ system, which was carried out by the method of quantum molecular dynamics at temperature values 800 °C–900 °C [1]. As a result of a series of numerical experiments, it was found that at such temperatures, already in the first tens of picoseconds, part of the layers of the adsorbed Ba-film left it, and this process continued until these temperatures impacted the film. At the same time, BaO- film did not peel off at such temperatures, which is due to the high value of the bond energy of the layers of this film relative to APG. This suggests that on the surface of APG, which acts as a grid material in CGK, most of the adsorbed material is barium oxide, and not barium. And, as a result, the work function of APG + adsorbates occurs due to the increased work function of „APG + BaO“ system equal to ~ 5.14 eV, which explains the absence of parasitic thermo-emission current observed in the experiment and, as a result, higher efficiency of CGK.

Conclusion

Experimental and theoretical studies have shown high anti-emission and strength properties of APG grids located near the emitting surface of MPC in the temperature range of grid electrodes 800 °C–900 °C at cathode temperatures 1080 °C–1150 °C. Molecular dynamic modeling using quantum mechanical density functional method demonstrated that APG work function in conditions of intense sputtering of evaporation products from the cathode rises up to ~ 5.14 eV. CGK tests in the device for 900 h at elevated temperature confirmed the absence of a parasitic thermo-emission current in the cathode-control grid circuit.

The use of CGKs in a high-power pulsed TWT will increase the reliability and durability of the high-power pulsed vacuum devices.

Conflict of interest

The authors declare that they have no conflict of interest.

Acknowledgment

The authors would like to thank A.V.Ushakov, Associate Professor of the Department of Physical Chemistry of Saratov State University for conducting the studies of APG sample lattice.

References

[1] R.Y. Bogachev, D.A. Bessonov, S.D. Zhuravlev, T.M. Krachkovskaya, V.I. Shesterkin. Elektronnaya tekhnika, Ser. 1. SVCh-tekhnika, **3** (563), 64 (2024 (in Russian).

[2] Yu.A. Grigoriev, B.S. Pravdin, V.I. Shesterkin. Obzory po elektronnoy tekhnike. Ser. 1. Elektronika SVCh., **7** (1246), 71 (1987) (in Russian).

[3] T.M. Gardiner. Intern. Conf. Microwave Tubes in Syst.: Problems Prospects, 1984.

[4] J. Jiang, B. Jiang, C. Ren, T. Feng, X. Wang, X. Liu, S. Zou. J. Vacuum Sci. Technol. A: Vacuum, Surfaces and Films, **23** (3), 506 (2005). DOI: 10.1116/1.1894726

[5] V.A. Smirnov, A.V. Konnov. Elektronnaya tekhnika. Ser. 1. SVCh-tekhnika, **2** (562), 23 (2024) (in Russian).

[6] I.P. Melnikova, A.V. Lyasnikova, S.V. Maltseva. Lett. Mater., **7** (3), 218 (2017). DOI: 10.22226/2410-3535-2017-3-218-221

[7] A. Shih, C.R.K. Marrian, G.A. Haas. In: Appl. Surf. Sci., **24**, 415 (1985).

[8] V.G. Kuznetsov, D.K. Kostrin. J. Phys.: Conf. Ser., **1954**, 1 (2021). DOI: 10.1088/1742-6596/1954/1/012026

[9] A. Latini, M. Tomellini, L. Lazzarini, G. Bertoni, D. Gazzoli, L. Bossa, D. Gozzi. PLOS ONE, **9** (8), 1 (2014). DOI: 10.1371/journal.pone.0105788

[10] M.K. De Pano, S.L. Hart, A.A. Hanna, A.C. Schneider. 40th AIAA/ASME/SAE/ASEE *Joint Propulsion Conference and Exhibit, Fort Lauderdale* (American Institute of Aeronautics and Astronautics Florida, USA, 2004), p. 1.

[11] J. Heikkinen, E. Petrola, N. Wester, J. Koskinen, T. Laurila, S. Franssila, V. Jokinen. Micromachines, **10** (510), 1 (2019). DOI: 10.3390/mi10080510

[12] V.I. Shesterkin, T.M. Krachkovskaya, P.D. Shalaev, L.T. Baymagambetova, S.D. Zhuravlev, D.I. Kirichenko, R.Yu. Bogachev. Radiotekhnika i elektronika, **67** (10), 1 (2022) (in Russian). DOI: 10.31857/S0033849422100102

[13] S.D. Zhuravlev, R.Yu. Bogachev, V.I. Rogovin, A.I. Petrosyan, V.I. Shesterkin, B.A. Grizbil, V.P. Ryabukho, A.A. Zakharov. Elektron. Tekh. Ser. 1, SVCh-Tekh., **4** (539), 45 (2018) (in Russian).

[14] D.A. Bessonov, R.Yu. Bogachev, S.D. Zhuravlev, T.M. Krachkovskaya, V.I. Shesterkin. *Sposob sovmestnoy proshivki dvoinykh setchatykh strukur metodom lazernoy ablyatsii* (Pat. № 2831606. Appl. (09.04.2024) (in Russian). Publ. 11.12.24)

[15] R.Y. Bogachev, D.A. Bessonov, S.D. Zhuravlev, T.M. Krachkovskaya, T.N. Sokolova, V.I. Shesterkin. *Sposob nerazyomnogo soedineniya detaley iz uglerodosoderzhaschykh materialov s detalyami iz metallov metodom lazernogo zaklepyvaniya* (Patent application № 2024105105 of 27.02.2024)

[16] J.M. Soler, E. Artacho, J.D. Gale, A. García, J. Junquera, P. Ordejión, D. Sánchez-Portal. J. Phys. Condensed Matter, **14** (11), 2745 (2002). DOI: 10.1088/0953-8984/14/11/302/

[17] J. Oroya, A. Martín, M. Callejo, M. García-Mota, F. Marchesin. *Pseudopotential and numerical atomic orbitals basis dataset*. In SIMUNE Atomistics (www.simuneatomistics.com)

[18] J.P. Perdew, K. Burke, M. Ernzerhof. Phys. Rev. Lett., **77** (18), 3865 (1996). DOI: 10.1103/PhysRevLett.77.3865

Translated by T.Zorina